Use of thermal imagery to assess temperature variation in ice collision processes

Jochen N.W.Tijsen
Memorial University Newfoundland
St. John's, Newfoundland, Canada
j.n.w.tijsen@gmail.com

S.E.Bruneau, B.Colbourne
Memorial University Newfoundland
St. John's, Newfoundland, Canada
sbruneau@mun.ca, bruce.colbourne@mun.ca

ABSTRACT
The paper describes the exploratory use of thermal imagery on ice collisional processes. This way of measuring provides a new source of information which may lead to new insights and improvements of existing ice collision models. Results indicate significant internal temperature rises in both the crushing case and in the sliding (friction) case. The paper provides some observations, however the main purpose is to show the value of applying thermal imagery in studies of collisional processes. Nevertheless the reader may be interested in the observations originating from the experiments. The first is that the internal temperature increments during ice friction are shown to track the trends in the friction coefficient. The second is that internal temperature increments during ice crushing appear to be concentrated in specific areas of the contact zone and may indicate high pressure zones.

KEY WORDS: Collision, friction, crushing, temperature, heat

INTRODUCTION

This paper describes an exploratory experimental program executed at Memorial University Newfoundland in the Fall 2013. The experiments are part of the multi-party research program STePS^2. The present program repeats some earlier crushing and friction experiments and adds a new measuring device to the experiment: A high quality thermal camera FLIR Ax5. The camera is very accurate and showed interesting results.
The purpose of the study was to provide preliminary data coming from the thermal camera on ice contact/crushing processes to determine if such measurements provided information of value. The thermal camera is able to measure temperature on the surface of the collision interface and the results will form the basis for follow-up research to more completely investigate thermal effects in ice contact zones. This paper shows the application of thermal imagery, but covers a few observations on friction and crushing. The observations are not definitive, but do show a new way of looking at the problem which may help to further explain contact phenomena like friction or crushing. Follow-up research is intended to correlate this new data to the existing data and theories. The background of thermal imagery can be found in Appendix B. The first part covers the frictional process and the second part covers the crushing process. Introductions to the two experimental setups are covered by each part separately.

ICE FRICTION

Experiment

The frictional experiments are conducted with standardized 25 cm diameter, 30 degree conical ice samples on a rotating plate. Details of the geometry, morphology and production process of the ice samples can be found in appendix A. The apparatus shown in Figure 1 comprises a large rotating table upon which an ice cone sample is lowered under constant vertical load. The sample is laterally restrained by a load cell as the table rotates at a constant rate. The apparatus is located inside a cold room kept at a constant temperature of -10C.

Figure 1 Setup friction experiment (Ice-ice friction)

Two sets of frictional tests have been conducted; One set is conducted with conical ice samples lowered onto a rotating ice surface and the second, the conical ice samples were lowered onto a rotating stainless steel plate with a sandblasted finish. The normal force (Fn), lateral

friction force (Ff), indentation depth (d) and the heat radiation (see Figure 2) are measured. The friction coefficient (μ) is computed directly from Fn/Ff.

The thermal camera was positioned at an oblique viewing angle 45 cm from the point of contact between the sample ice cone and the rotating surface. The temperatures of all surfaces (including equipment load cells etc.) in the viewing window were observed to fall within the range of -10.5 - -14.5 C prior to contact. As the cone was lowered, contact was made and the cone tip was sheared down as the weight was fully applied. The contact pathway inscribed on the lower plate was circular and continuously over-ridden by the cone with each successive rotation. The debris from the cone tip crushing was swept clear of the surface before returning to the contact area. Eventually equilibrium was approached in which neither surface lost much material and the frictional force stabilized.

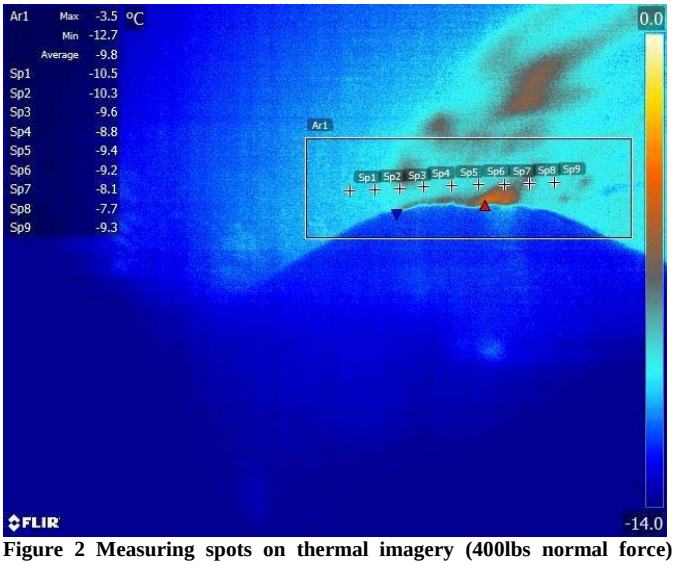

Figure 2 Measuring spots on thermal imagery (400lbs normal force) – upside down compared to the setup

The thermal image record of this experiment was scrutinized and revealed an appreciable heating of the rotating ice surface as it emerged from underneath the contact zone. Figure 2 is a single frame of the 30fps contact video. In that figure one can observe the ice temperature ranging from the ambient -14C (dark blue) far from the contact zone up to as high as -7 (orange) within and extremes of -3.5 (light orange) close to the curved arc of the pathway over which the cone has recently passed. The rotational speed of the machine was 23 RPM and the radius at which contact was made was 37 cm thus the differential speed at the centre of contact was 0.14 m/s and the period of rotation was 2.6 seconds.

The contact pathway revealed an uneven distribution of temperatures spatially and temporally. Zones of high temperature appear to emerge in a scattered pattern across the width of the path. The elevated temperatures fall back quickly so that the temperature of the pathway re-entering the contact zone is up to 8 degrees above the surrounding un-touched ice. The analysis software enabled easy point sampling of temperatures and thus a simple section of the pathway was sampled at 9 points to yield a profile. In subsequent tests, performed at higher normal loads the thermal record revealed increasing trends.

Behavior of the frictional temperatures

The effect of temperature on the friction coefficient is previously described by Slotfeldt-Ellingsen & Torgersen, 1983, Tusima, 1977 and Kietzig et al., 2010. The temperature considered in their research is the environmental temperature, in other words the external temperature. See Figure 3 for the relation between temperature and friction coefficient. The temperature considered in this paper is the internal temperature as it is influenced by frictional heat. However, the effect on the friction coefficient could be similar.

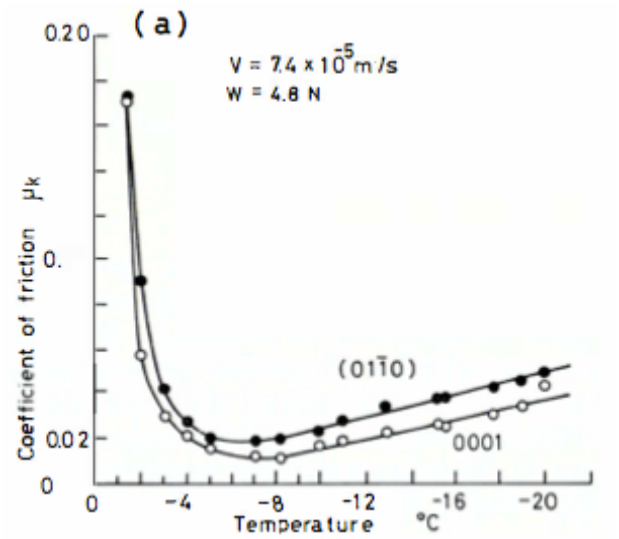

Figure 3 Effect of Temperature on the Friction Coefficient, ice-steel friction [Tusima, 1977]

The friction coefficient seems to increase when the temperature is approaching 0 Celsius according to Tusima, 1977. This paper presumes a certain interaction between the internal temperature (local spot 5 at the observed path of the ice cone on the rotating plate) and the friction coefficient. The time history of both is shown for a sample test in Figure 4

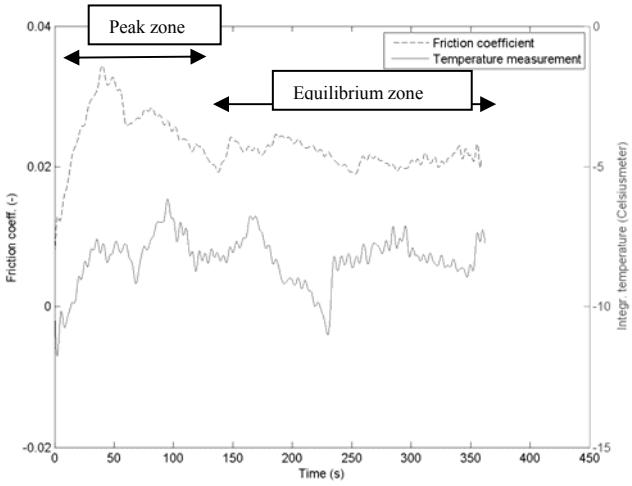

Figure 4 Friction coeff. vs. temperature ice-ice friction (400lbs normal force)

Figure 4 shows the temperature measurement of location number 5 in Figure 2. The sensitivity of one local spot is much higher than averaged over the track width. However, in order to represent the graph as an overall temperature (global temperature action) one should make the

active track width as a function of the indentation depth. The measurements of both friction and temperature are filtered (Low pass filter: 0 – 0.2 Hz) in order to reveal trends in the results. However, local extreme temperatures may be important in the correlation between the friction coefficient and temperature.

Two zones in the timespan of the frictional coefficient are observed:

i) Peak zone after starting the experiment.

ii) Equilibrium zone, a transient part where the temperature tends to approach equilibrium.

The first part of the measured temperatures seems to behave similarly to the friction coefficient. Both are achieving a peak, the peak temperature is dependent on several factors, but achieved very high temperatures up to -3.5 degrees Celsius for 400lbs normal force. The friction coefficient seems to reach a peak as well at about the same time. The peak temperatures are observed very locally and not continuously, but might contribute to the peak friction coefficient. The trend that increasing external temperatures increase the friction coefficient are confirmed by results shown in Figure 3 and that relation may be plausible for the internal temperature and friction coefficient too.

The second part of the timespan seems to be stabilizing for both temperatures and friction coefficient. Determining the mass, impulse and energy balance in further research might contribute to a more detailed description of the equilibrium zone.

Influence of normal weight

The experiment covered four normal force levels. The friction force increases proportional to the normal force. Figure 5 illustrates the behavior of the temperatures for the normal force levels 200lbs and 400lbs:

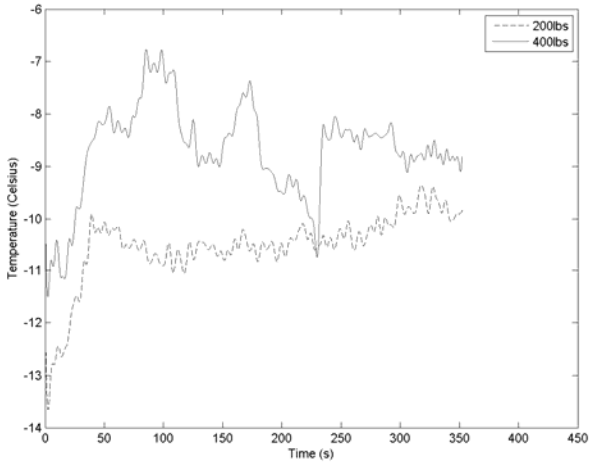

Figure 5 Influence of normal weight on temperature for ice-ice friction

The temperature difference seems to indicate an increment in global temperature with increasing normal weight. The temperature increment is expected due to an increasing amount of work delivered by the friction force. Oksanen & Keinonen, 1982 and Albracht et al., 2004 describe the effect of decreasing friction coefficient (to a limiting value) by increasing normal force, depicted in Figure 6.

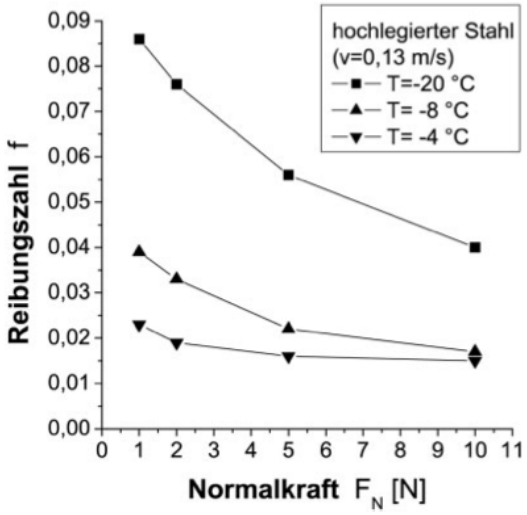

Figure 6 Effect of Normal Force on the Friction Coefficient with Different Temperatures, ice-steel friction [Albracht et al., 2004] and [Dagenais, 2013]

The internal equilibrium temperature increases for increasing normal weight. The explanation could be that the internal temperature for increasing normal weight, is also increasing, and approaches the temperature of the minimum friction coefficient (as is seen in Figure 3) and may contribute to the reduction of the friction coefficient.

Influence of speed level

The data reveals an interesting anomaly, an asymmetrical average of the measured temperatures over the track width. The anomaly could be explained by the small difference in speed of the side towards the center of the rotating disc and the outer side. That might mean an increasing speed level would result in increasing energy dissipation in the form of heat and measured as internal temperature. This seems plausible when considering the extra amount of delivered work of the friction force. The asymmetrical average is depicted in Figure 7.

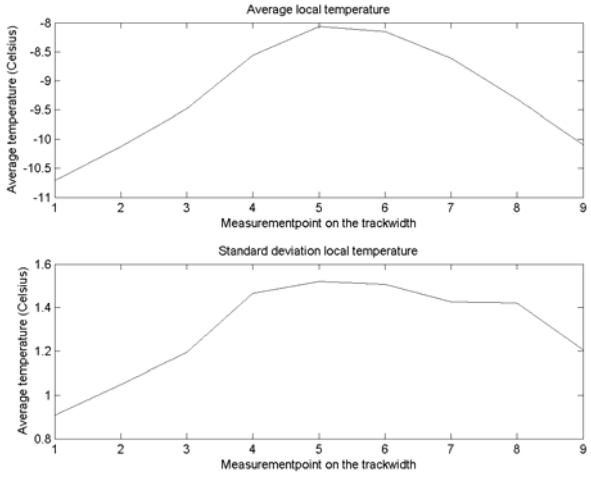

Figure 7 Statistical data temperatures over track width (Ice-ice 400lbs)

The chance does still exist that the asymmetry is a product of inaccuracy in the positioning of the measurement spots as is seen in Figure 2. In order to make a stronger statement about the influence of speed on the heat generation, the experiments should be reproduced in higher experiment numbers and with larger speed differences.

Influence of material difference

The friction experiment is conducted for both ice-ice and ice-steel contact conditions. The difference between ice friction on steel and on ice is not just one factor. Several material related factors differ such as roughness, thermal conductivity and wettability.

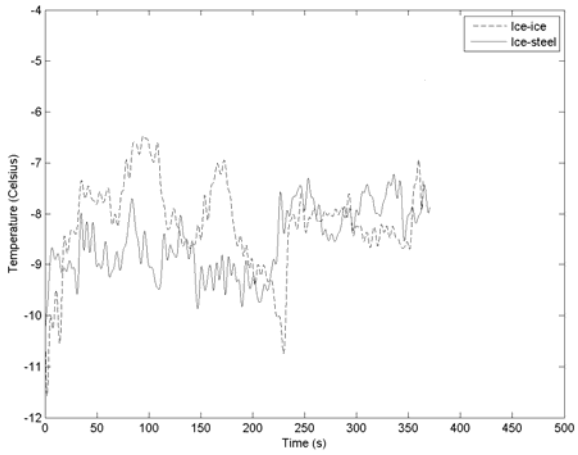

Figure 8 Influence of material differences (400lbs)

Figure 7 shows that for ice-steel friction, there is a high frequency variation in temperature. The data shows that the heat dissipates faster at the sandblasted steel than at the ice interface by the high frequency variation. The higher thermal conductivity is thought to be a cause for this effect.

ICE CRUSHING

Experiment

The crushing experiment involves crushing a standardized 25 cm diameter, 30 degree conical sample against a rigid steel plate in both ductile and brittle speed ranges, using an MTS machine in a large cold room. The temperature in the cold room is maintained at -10 Celsius. The MTS machine may be configured for variable speed levels. High and low speed levels are used for the purpose of the exploratory research. The normal force is measured by load cells (see Figure 9). The thermal camera is positioned sideways in order to record the surface temperatures of the spalls, crushing interface and ice contact area after lifting the crushing plate (see Figure 11 and Figure 13). The set-up is shown in Figure 9 and Figure 10.

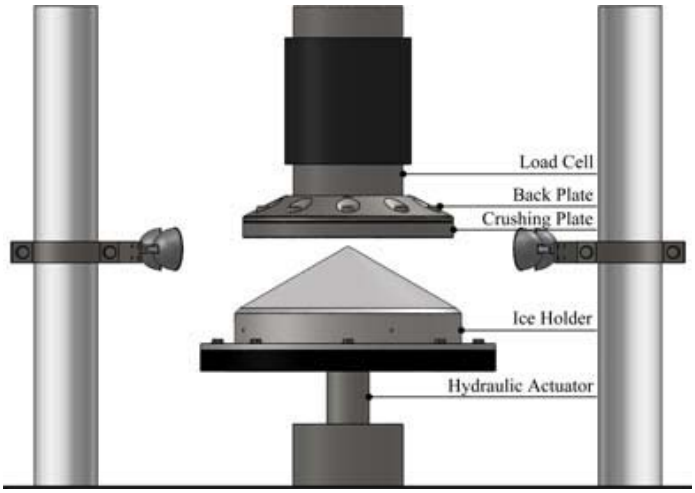

Figure 9 Schematic of the crushing test [Dragt, 2013]

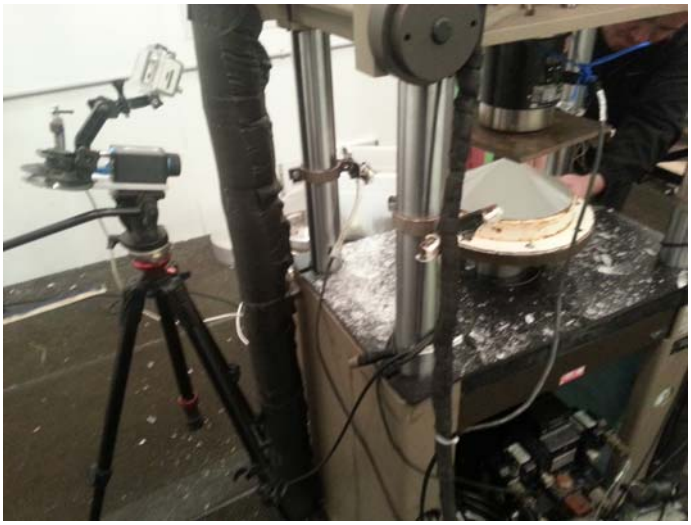

Figure 10 Setup crushing experiment

Ductile and brittle crushing

Low crushing speeds at 0.1 mm/s can not give any significant results on the thermal imagery, because any heat which is generated will dissipate faster than can be observed. However for brittle crushing speeds (>10 – 100 mm/s) some significant temperature increments were observed. The main interest is the origin of the spalls and how thermodynamic and mechanic phenomenon on the ice crushing interface interact with each other.

Crushing heat spots

The crushing heat spots can be recognized very well after lifting the crushing plate. The lift of the crushing plate takes a few seconds in which the heat dissipates quickly, so the spots are probably warmer than depicted in Figure 11.

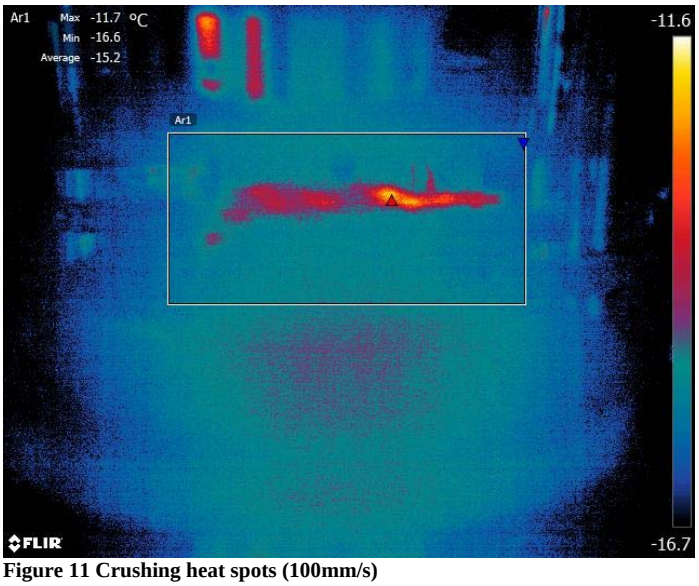

Figure 11 Crushing heat spots (100mm/s)

The strength of ice is strongly dependent on the high pressure zones at the crushing interface, illustrated by **Figure 12**. One is probably able to identify high pressure zones by finding the crushing heat spots. The relation seems plausible considered the amount of work done by the crushing force divided over the crushing area of the ice.

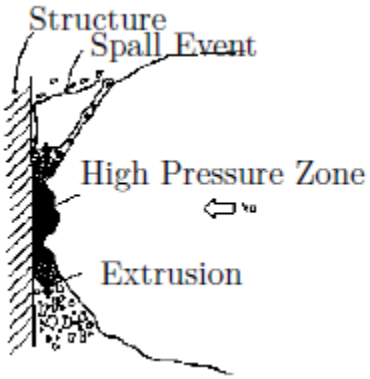

Figure 12 Schematic of a critical zone with spalls [Zou et al., 1996] and [Dragt, 2013]

Temperature spalls

Brittle crushing generates spalls which flake off the parent ice. The spalls appear to show a significant temperature increment up to 8.2 degrees Celsius (even after a 1 second cooling time). The origin of the spalls could indicate the location of the crushing heat spots and probably the high pressure zones. Figure 13 shows the temperature increment of a spall.

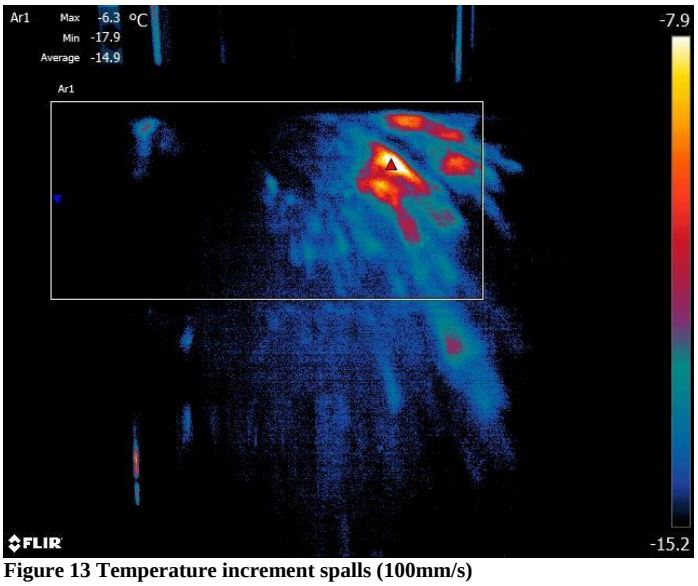

Figure 13 Temperature increment spalls (100mm/s)

CONCLUSIONS AND RECOMMENDATIONS

The major conclusion of this preliminary study is that the use of a thermal camera provides a new rich source of information about ice contact/collision processes. The thermal camera gives the observer a different perspective and clues about the involvement of heat during contact events. The discovered temperature increments during both friction and crushing phenomena leads to a number of follow-up questions, all related to what degree do the thermodynamic and mechanical behavior of friction and crushing interact? Answers to these questions could lead to a better understanding of the friction and crushing models of ice and possibly to new measuring technology for ice collisional loads. Follow-up research is planned to address this and other issues. The work will consist of similar experiments with higher loads and more series of these experiments are planned in order to make better justified conclusions and statements. The ultimate aim is to develop a model which relates measured temperatures to heat generative processes and then link these models to observations of pressure and friction coefficient.

ACKNOWLEDGEMENTS

The authors are thankful to the STePS^2 group and partners. Special thanks goes to the RAVEN group of the Memorial University Newfoundland which provided the camera and assistance in the thermal camera operations. Without them the research wouldn't be possible.

REFERENCES

ALBRACHT, F., REICHEL, S., WINKLER, V. and KERN, H., 2004. On the Influences of Friction on Ice. *Materialwissenschaft und Werkstofftechnik,* 35(10-11), pp. 620-625.

DAGENAIS, J, 2013. Effects of normal force, velocity and lubrication on ice friction at high pressures, chapter 1.

DRAGT, R., 2013. The collision of cone-shape ice samples against steel plates of varying surface roughness, chapter 2.

KIETZIG, A.M., 2010. *Microscopic Ice Friction*, The University of British Columbia.

OKSANEN, P. and KEINONEN, J., 1982. The Mechanism of Friction of Ice. *Wear,* **78**(3), pp. 315-324.

SLOTFELDT-ELLINGSEN, D. and TORGERSEN, L., 1983. Water on Ice; Influence on Friction. *Journal of physics.D, Applied physics,* **16**(9), pp. 1715-1719.
TUSIMA, K., 1977. Friction of a Steel Ball on a Single Crystals of Ice. **19**(81), pp. 225-235.

APPENDIX A: ICE MAKING PROCEDURE

The purpose of the ice making procedure is to make ice with a consistent, reproducible set of mechanical properties which is also an reasonable reflection of natural ice. The process has been described by Bruneau et al., 2012. The ice sample is made of sieved ice grains, from 4 – 10+ mm and treated water. The ice grain size distribution is consistent for all ice samples. The distribution has not been analyzed for the exploratory character of the paper, but should be consistent over the experimental program due to careful sieving procedures.

The water is distillated, deionized, de-aerated and chilled to approximately 0 degrees Celsius before mixing. After addition in the bucket (in the freezer) the ice is thoroughly shaken to compact it and topped off with treated water. **Figure 14** shows the schematic of the unidirectional growth of ice samples. Unidirectional growth reduces the risk on high internal stresses and cracks.

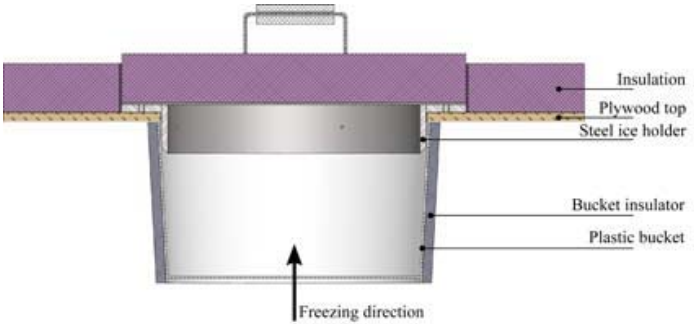

Figure 14 Unidirectional growth of ice samples

The last step is the shaping of the ice sample to a cone form (30 degree cone angle), this is done by an ice shaping apparatus. The apparatus uses a rotating plate and a blade to shape slowly the cone. The main concern is to minimize the internal stresses and the risk on cracks in the sample.

APPENDIX B: THERMAL IMAGERY

The type Ax5 FLIR high quality thermal camera has been used. The specification of the camera won't be discussed here, but one can find them on the FLIR website. The thermal camera is able to record infrared radiation as is seen in the spectrum in **Figure 15**:

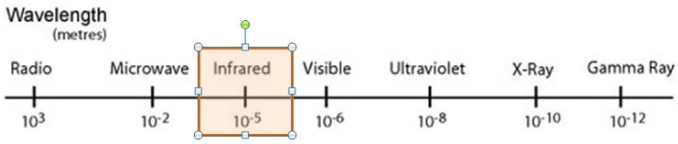

Figure 15 Infrared in the electromagnetic spectrum

The technology is able to measure infrared radiation and calculate the surface temperatures of materials. The technology makes use of the blackbody theory. The ideal blackbody is defined as an object which absorbs all radiation that impinges on it at any wavelength. The phenomenon described in **Figure 16** is researched by Planck (1858 – 1947).

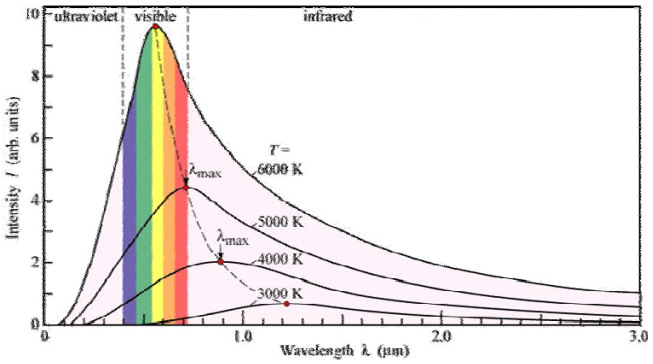

Figure 16 Blackbody radiation

Planck's formula is only valid for blackbody radiation and imply the relation in the derivative between temperature and wavelength. The maximum intensity of each temperature is dependent on the wavelength and is given by the following formula:

$\Lambda_{max} = 2898/T;$

Where,

T : Temperature (Kelvin)
Λ_{max} : Wavelength with maximum intensity (μm)

The infrared radiation measured by the camera is unfortunately not only blackbody radiation. The following radiative sources are observed:

- Black body radiation (true temperature)
- Reflective radiation
- Transmitting radiation

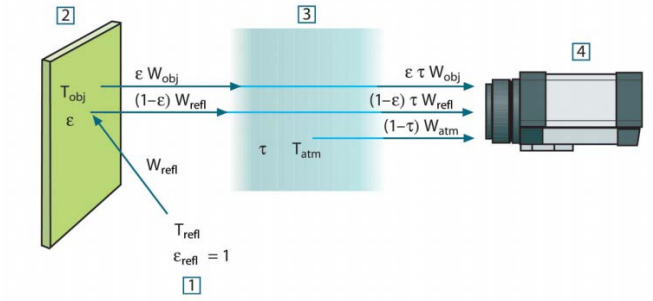

Figure 17 Radiation sources [FLIR Tool+ manual]

Figure 17 shows schematic from object to camera the radiative heat intensity of heat sources. The object does radiate (nr. 2) and reflect radiation (nr. 1), a correction is applied by the coefficient epsilon. The coefficient may be determined by a calibration test and is explained in more detail on the FLIR website. The reflective correction has not been applied in this paper (epsilon = 1), because all potential heat sources have been carefully taken away prior to testing. The second correction is on the transmittance or in other words the absorption of the medium where the radiation is traveling through (3), most of the times air. The transmittance correction has not been applied in this paper, because the distance between camera and object (the ice cone tip) was small (40 – 140 cm).

The FLIR software is very accessible and able to post process the thermal imagery. The software had definitely contributed to the great quality imagery and detailed measurements. However, in order to confirm the quantitative temperature results calibration tests need to be applied as an extra quality check.